

# Chiral Fermions on the Lattice

Robert G. Edwards, Urs M. Heller and Rajamani Narayanan

*SCRI, The Florida State University, Tallahassee, FL 32306-4130, USA*

## Abstract

The Overlap-Dirac operator provides a lattice regularization of massless vector gauge theories with an exact chiral symmetry. Practical implementations of this operator and recent results in quenched QCD using this Overlap-Dirac operator are reviewed.

## 1 Introduction

Since the beginning of lattice gauge theory the regularization of chiral fermions has been afflicted with severe problems. When regulating fermions on a lattice, typically, unwanted doublers with opposite chirality appear. These doublers can be lifted (given mass of the order of the cut-off) at the cost of explicitly breaking chiral symmetry, as in the Wilson fermion formulation. Alternatively, a remnant of chiral symmetry can be retained, with a smaller number of doublers interpreted as flavors, as in the staggered fermion formalism. However, at finite lattice spacing the flavor symmetry is broken. Both these approaches fail from the outset for regulating Weyl fermions. The central problem in the non-perturbative regularization of gauge theories with Weyl fermions is to write down a formula for the fermionic determinant when the fermion is in some complex representation of the gauge group, since depending on the topology of the gauge field the chiral Dirac operator can be square or rectangular, where the difference between rows and columns is the index.

Significant progress in the formulation of chiral gauge theories has been made by the overlap formalism [1]. The overlap formalism was inspired by two papers [2]. The central idea is that an infinite number of Dirac fermions (labeled by  $s$ ) with a mass term of the form  $\bar{\psi}_s(P_L M_{ss'} + P_R M_{ss'}^\dagger)\psi_{s'}$  and chiral projectors  $P_{L,R}$  can be used to regulate a single Weyl fermion if the infinite dimensional mass matrix  $M$  has a single zero mode but  $M^\dagger$  has no zero modes. Kaplan's paper [2] uses this idea to put chiral fermions on the lattice

where they are referred to as domain wall fermions since Kaplan used a mass matrix that has a domain wall like structure. In the overlap formalism the infinite number of Dirac fermions is described by two non-interacting many body Hamiltonians, one for each side of the domain wall, and the chiral determinant is written as the overlap between their groundstates

$$\det C(U) \Leftrightarrow \langle 0- | 0+ \rangle. \quad (1)$$

$|0-\rangle$  is the many body ground state of  $\mathcal{H}^- = a^\dagger \gamma_5 a$  and  $|0+\rangle$  the many body ground state of  $\mathcal{H}^+ = a^\dagger H_w(U) a$ , with  $\gamma_5 H_w(U) = D_w(U)$  the usual Wilson-Dirac operator on the lattice with a fermion mass in the supercritical region ( $m_c < m < 2$ ).  $a$  ( $a^\dagger$ ) are canonical fermion annihilation (creation) operators. On a finite lattice, the single particle Hamiltonians are finite matrices of size  $2K \times 2K$  with  $K = V \times N \times S$  where  $V$  is the volume of the lattice,  $N$  is the size of the particular representation of the gauge group and  $S$  is the number of components of a Weyl spinor. Then  $|0-\rangle$  is made up of  $K$  particles. If  $|0+\rangle$  is also made up of  $K$  particles, then the overlap is not zero in the generic case. If the background gauge field is such that there are only  $K - Q$  negative energy states for  $H_w(U)$  then the overlap is zero. Any small perturbation of the gauge field will not alter this situation. Furthermore, the overlap  $\langle 0- | a_{i_1}^\dagger \cdots a_{i_Q}^\dagger | 0+ \rangle$  will not be zero in the generic case if the fermion is in the fundamental representation of the gauge group showing that there is a violation of fermion number by  $Q$  units. So, clearly, the overlap definition of the chiral determinant (1) has the desired properties.

A generic problem with simulations of chiral gauge theories is that the chiral fermion determinant is complex. A “brute force approach” is feasible in the simulation of two dimensional models, and in this way the overlap formalism has successfully reproduced non-trivial results in two dimensional chiral models on the lattice [3]. The brute force approach, however, is clearly not feasible in four dimensions, where efficient numerical techniques are essential. This prevented simulations of chiral gauge theories and tests of the overlap formalism in four dimensions so far.

Clearly, any formulation of lattice chiral gauge theories is also a formulation of massless vector gauge theories with an exact chiral symmetry and a positive fermion determinant (the product of the chiral determinant for the left handed fermions and its complex conjugate for the right handed ones). Lattice QCD using the overlap formalism reproduces the well-known mass inequalities between mesons and baryons, and the  $U(N_f)_V \times U(N_f)_A$  symmetry in an  $N_f$  flavor theory is broken down to  $U(1)_V \times SU(N_f)_V \times SU(N_f)_A$  by gauge fields that carry topological charge [4]<sup>1</sup>. If the  $SU(N_f)_V \times SU(N_f)_A$  symmetry is spontaneously broken, then massless Goldstone bosons should naturally

---

<sup>1</sup> See section 9 of [1] for details.

emerge in the overlap formalism. Since the symmetry breaking pattern is exactly as in the continuum, all the soft pion theorems should hold on the lattice as well.

For a vector gauge theory the computation of the fermionic determinant can be simplified significantly compared to the original version (1) that involves the computation of the overlap of two many body ground states. One way to derive the simplified expression is to start with the variant of domain wall fermions of ref. [5], applicable for a vector gauge theory. We choose this approach here to emphasize the close connection between domain wall and overlap fermions. Integrating out all the fermion and Pauli-Villars fields, Neuberger derived the following expression for the determinant describing a single light Dirac fermion [6]

$$\det D_{DW}(\mu; L_s) = \det \left\{ \frac{1}{2} \left[ 1 + \mu + (1 - \mu) \gamma_5 \tanh \left( -\frac{L_s}{2} \ln T_w \right) \right] \right\}. \quad (2)$$

Here  $T_w$  is the transfer matrix in the extra direction, whose extent,  $L_s$ , has been kept finite, and  $0 \leq \mu \leq 1$  describes fermions with positive mass all the way from zero to infinity. In [5] the fermion mass  $\mu$  is denoted by  $m_f$ . In the limit  $L_s \rightarrow \infty$  (2) becomes

$$\det D_{DW}(\mu) = \det \left\{ \frac{1}{2} [1 + \mu + (1 - \mu) \gamma_5 \epsilon(-\ln T_w)] \right\}. \quad (3)$$

It is only in this limit that massless domain wall fermions have an exact chiral symmetry. Finally, taking the lattice spacing,  $a_s$ , in the extra direction to zero one obtains the Overlap-Dirac operator of Neuberger [7]

$$D(\mu) = \frac{1}{2} [1 + \mu + (1 - \mu) \gamma_5 \epsilon(H_w)]. \quad (4)$$

The external fermion propagator is given by

$$\tilde{D}^{-1}(\mu) = (1 - \mu)^{-1} [D^{-1}(\mu) - 1]. \quad (5)$$

The subtraction at  $\mu = 0$  is evident from the original overlap formalism [1] and the massless propagator anti-commutes with  $\gamma_5$  [4,7]. With our choice of subtraction and overall normalization the propagator satisfies the relation

$$\mu \langle b^\dagger | [\gamma_5 \tilde{D}^{-1}(\mu)]^2 | b \rangle = \langle b^\dagger | \tilde{D}^{-1}(\mu) | b \rangle \quad \forall b \text{ satisfying } \gamma_5 |b\rangle = \pm |b\rangle \quad (6)$$

for all values of  $\mu$  in an arbitrary gauge field background [8]. The fermion

propagator on the lattice is related to the continuum propagator for small momenta and small  $\mu$  by

$$D_c^{-1}(m_q) = Z_\psi^{-1} \tilde{D}^{-1}(\mu) \quad \text{with} \quad m_q = Z_m^{-1} \mu \quad (7)$$

where  $Z_m$  and  $Z_\psi$  are the mass and wavefunction renormalizations, respectively. Requiring that (6) hold in the continuum results in  $Z_\psi Z_m = 1$ . We find that a tree level tadpole improved estimate gives

$$Z_\psi = Z_m^{-1} = \frac{2}{u_0} [m - 4(1 - u_0)] , \quad (8)$$

where  $u_0$  is one's favorite choice for the tadpole link value. Most consistently, for the above relation, it is obtained from  $m_c$ , the critical mass of usual Wilson fermion spectroscopy.

In the rest of this paper we discuss practical implementations of the Overlap-Dirac operator and present some recent results. Owing to the recent flurry [9] of theoretical activity arising from the “unearthing” of the Ginsparg-Wilson relation [10], a few remarks are in order. The massless Overlap-Dirac operator in (4) satisfies the Ginsparg-Wilson relation

$$D(0)\gamma_5 + \gamma_5 D(0) = 2D(0)\gamma_5 D(0) \quad (9)$$

implying that the massless propagator  $(D^{-1}(0) - 1)$  anticommutes with  $\gamma_5$ . If we write

$$D(0) = \frac{1}{2} [1 + \gamma_5 \hat{H}_a] . \quad (10)$$

then the Ginsparg-Wilson relation reduces to  $\hat{H}_a^2 = 1$ . Since we would want  $\gamma_5 D(0)$  to be Hermitian,  $\hat{H}_a$  should be a Hermitian operator. With this reduction of the Ginsparg-Wilson relation, it is easy to show that [11]

$$\det D(0) = |\langle 0 - | 0+ \rangle|^2 \quad (11)$$

*i.e.*, the overlap formula for a vector theory. Here  $|0+\rangle$  is the many body ground state of  $a^\dagger \hat{H}_a a$ . This establishes a one-to-one correspondence between the overlap formula and the determinant of a fermionic operator satisfying the Ginsparg-Wilson relation for massless vector gauge theories.

## 2 Practical Implementations of $\epsilon(H_w)$

In order to compute the action of  $\epsilon(H_w) = \frac{H_w}{|H_w|}$  on a vector one can proceed in several different ways. Since we are interested in working in four dimensions, it is not practical to store the whole matrix  $H_w$ . Therefore standard techniques to deal with the square root of a matrix [12] will not be discussed.

One could attempt to solve the equation  $\sqrt{H_w^2}\phi = H_w b$  to obtain  $\phi = \epsilon(H_w)b$  using iterative techniques. Such techniques have been developed to solve linear systems with fractional powers of a positive definite operator using Gegenbauer polynomials [13] and applied to the Overlap-Dirac operator in [14].

Another approach is to efficiently approximate  $\epsilon(H_w)$  as a sum of poles:

$$\epsilon(H_w) \approx g_N(H_w) = H_w \left[ c_0 + \sum_{k=1}^N \frac{c_k}{H_w^2 + d_k} \right]. \quad (12)$$

The action of  $\epsilon(H_w)$  on a vector then involves a single conjugate gradient with multiple shifts [15].

One approximation, called the polar decomposition [16], has been adapted in this context and first used in the study of the three dimensional Overlap-Dirac operator by Neuberger [17]. Here the coefficient  $c_0 = 0$  and

$$c_k = \frac{1}{N \cos^2 \frac{\pi}{4N}(2k-1)}; \quad d_k = \tan^2 \frac{\pi}{4N}(2k-1). \quad (13)$$

In this approximation,

$$\epsilon(z) \approx g_N(z) = \frac{(1+z)^{2N} - (1-z)^{2N}}{(1+z)^{2N} + (1-z)^{2N}}. \quad (14)$$

Clearly  $g_N(z) = g_N(1/z)$  and  $g_N(1) = 1$ . The error  $\epsilon(z) - g_N(z)$  is strictly positive and monotonically decreases from  $z = 0$  to  $z = 1$ .

For another approximation, called the optimal rational approximation [18], the coefficients are obtained numerically by an optimal fit using the Remez algorithm. The coefficients in a slightly different notation have been tabulated for  $N = 6, 8, 10$  in Ref. [14]. We have found it necessary to use  $N = 14$  for our recent applications. The coefficients in this case are shown in Table 1. In the optimal rational approximation, the approximation to  $\epsilon(z)$  has oscillations and is not bounded by unity. A plot of the approximation  $g_N(z)$  obtained as a fit over the region  $[0.001, 1]$  is shown in Fig. 1 for  $N = 6$  to 14. While we fit

(2.413330975e+00,1.361747338e+01)	(6.257184884e-01,3.135687028e+00)
(2.925707925e-01,1.213113539e+00)	(1.737405612e-01,5.596349298e-01)
(1.166359792e-01,2.752627333e-01)	(8.372555094e-02,1.364115846e-01)
(6.216038074e-02,6.543005714e-02)	(4.652496186e-02,2.923946484e-02)
(3.423610040e-02,1.164228894e-02)	(2.404754621e-02,3.887745892e-03)
(1.545550091e-02,9.937321442e-04)	(8.436481876e-03,1.684882417e-04)
(3.419245947e-03,1.585925699e-05)	(1.138166539e-03,5.914114023e-07)

Table 1

The coefficient pairs  $(c_k, d_k)$   $k = 1, \dots, N$  for the  $N = 14$  optimal rational approximation for which  $c_0 = 0.0850910$ . The coefficients are obtained as a result of an optimal fit over the interval  $[0.001, 1]$ .

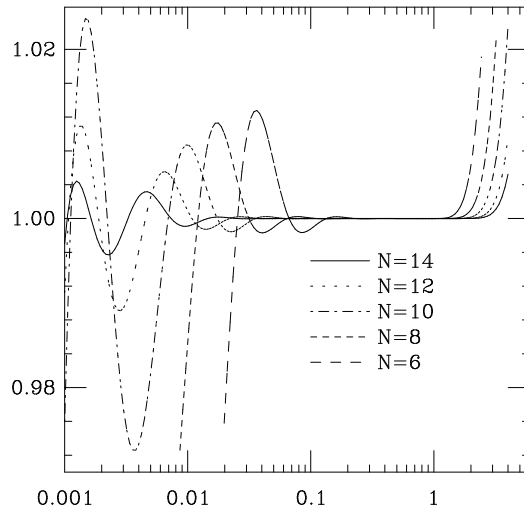


Fig. 1. Plots of the optimal rational function approximation to  $\epsilon(z)$  (Eq. 12) over the interval  $[0.001, 1]$  for  $N = 6, 8, 10, 12$ , and  $14$ . The small  $z$  region of  $N = 6$  and  $8$  is not shown. The fits are still good for some  $z > 1$ .

over this region, the approximation is still good for  $z$  somewhat larger than 1. The approximation is bounded by unity only if  $0.025 < z < 1.918$  for  $N = 14$ . In this range the maximum deviation from unity is equal to  $3.1 \times 10^{-5}$ . This range will increase if one increases the order of the approximation. For the current applications we found this range to be sufficient.

The approximation to  $\epsilon(H_w)$  by poles involves a multi-shift inner conjugate gradient and therefore it seems necessary to store  $N$  vectors where  $N$  is the order of the approximation. One can avoid storing the extra vectors if one is willing to perform two passes of the inner conjugate gradient [19]. A Lanczos based algorithm that also avoids this extra storage by requiring two passes

has been proposed, but it involves an explicit diagonalization of a tridiagonal matrix [20]. In this method  $H_w$  is approximated by a small dimensional tridiagonal matrix (anywhere between 100 and 1000) and  $\epsilon(H_w)$  is computed by first diagonalizing the tridiagonal matrix and then performing the trivial operation of  $\epsilon$  on the eigenvalues. The accuracy is increased by increasing the order of the tridiagonal matrix.

Since in practice it is the action of  $D(\mu)$  on a vector we need, we can check for the convergence of the complete operator at each inner iteration of  $\epsilon(H_w)$ . This saves some small amount of work at  $\mu = 0$  and more and more as  $\mu$  increases, while at  $\mu = 1$  (corresponding to infinitely heavy fermions, c.f. Eq.(4)) no work at all is required.

Each action of  $\epsilon(H_w)$  involves several applications of  $H_w$  on a vector with the number depending on the condition number of  $H_w(m)$  in the supercritical mass region. In Figure 2 we show the density of (near) zero eigenvalues for  $m = 1.7$ . We see that while  $\rho(0; 1.7)$  decreases rapidly as  $\beta$  increases, it does not appear to go zero at a finite lattice spacing. The second part of Figure 2 emphasizes that  $\rho(0; 1.7)$  decreases exponentially in some power of  $1/a$  (the power here is not well determined, but reasonably fits  $1/2$ ). This result implies that on a specific gauge background,  $H_w$  could have an arbitrarily large condition number due to a few small eigenvalues. This can make the computation of  $\phi = \epsilon(H_w)b$  expensive for all methods considered. In addition some care is needed when using the approximation of  $\epsilon(H_w)$  by a sum over poles. Clearly  $\epsilon(H_w)$  can be replaced by  $\epsilon(sH_w)$  where  $s > 0$  is an arbitrary scale factor. We should choose the scale so that the maximum eigenvalue of  $sH_w$  is not above the range where the approximation is deemed good. Having so chosen a value for  $s$ , we need to deal with the low lying eigenvalues that fall outside the range of the approximation to  $\epsilon(H_w)$ . We do this by computing a few low lying eigenvalues and eigenvectors of  $H_w$ , for which we then know the contribution to  $\epsilon(H_w)$  exactly, and projecting them out before applying the approximation to the orthogonal subspace for which the approximation is good. The number of eigenvalues that have to be projected out will depend on the lattice coupling, the lattice size and the lower end of the range of the approximation. It will roughly increase with the volume at a fixed coupling making it difficult to go to large lattice volumes at strong coupling. However, the number of eigenvalues that have to be projected out will decrease as one goes to weaker coupling even at a fixed physical volume. This is because the density of eigenvalues of  $H_w$  near zero goes to zero as one goes to the continuum limit [21]. The Ritz functional method [22] can be used to efficiently compute the necessary low lying eigenvalues and eigenvectors of  $H_w$ .

For the case of domain wall fermions at finite extent  $L_s$  in the fifth direction, the degree to which  $\tanh(-L_s(\ln T_w(m))/2)$  approximates  $\epsilon(-\ln T_w(m))$  is determined by  $L_s$  and the eigenvalues of  $T_w(m)$  near 1. One can show ana-

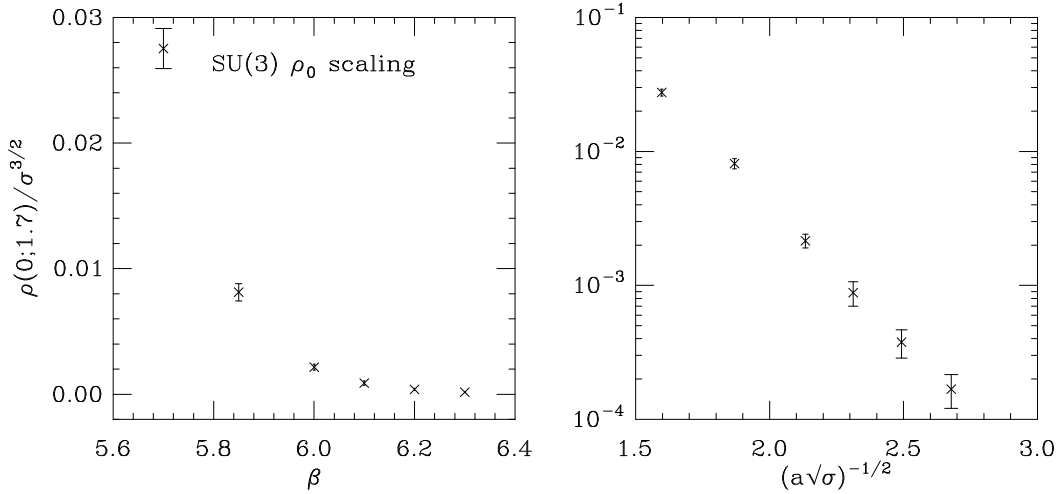


Fig. 2. The approach of  $\rho(0; 1.7)$  to the continuum limit versus  $\beta$  and versus  $1/\sqrt{a^2\sigma}$ .

lytically [1] that in a fixed gauge background a unit eigenvalue of  $T_w(m)$  and a zero eigenvalue of  $H_w(m)$  occur at the same mass  $m$ . Also, the change of the corresponding eigenvalue in  $m$  is the same for both  $T_w(m)$  and  $H_w(m)$ . This implies that the density of zero eigenvalues  $\rho(0; m)$  is the same for both  $H_w(m)$  and  $-\ln(T_w(m))$ . The degree to which these zero eigenvalues affect physical results is determined by the physical observable,  $L_s$ , and the fermion mass  $\mu$ . Studies of the  $L_s$  dependence for various quantities at non-zero fermion masses can be found in Ref. [23]. In particular, larger  $L_s$  at fixed mass  $\mu$  is needed for stronger coupling due to the increasing  $\rho(0; m)$ .

### 3 Spontaneous chiral symmetry breaking

Spontaneous chiral symmetry breaking is an important feature of QCD. However, it is not fully realized on a finite lattice and at finite quark mass. Thus one needs to carefully study the approach to the infinite volume and chiral limit. Conventional lattice fermion formulations explicitly break the chiral symmetry (at least partially) at finite lattice spacing, obscuring the approach to the infinite volume and chiral limit in practical simulations. Overlap fermions preserve the chiral symmetry at finite lattice spacing. This should facilitate a study of spontaneous chiral symmetry breaking. As a practical test of the Overlap-Dirac operator, we consider quenched QCD. The chiral limit of quenched QCD is tricky, though, because topologically non-trivial gauge fields are not suppressed in this limit. Gauge field topology results in exact zero modes of  $D(0)$  as long as one is in the supercritical region of  $H_w(m)$ . This is demonstrated in Fig. 3 where we show the spectral flow of eigenvalues of

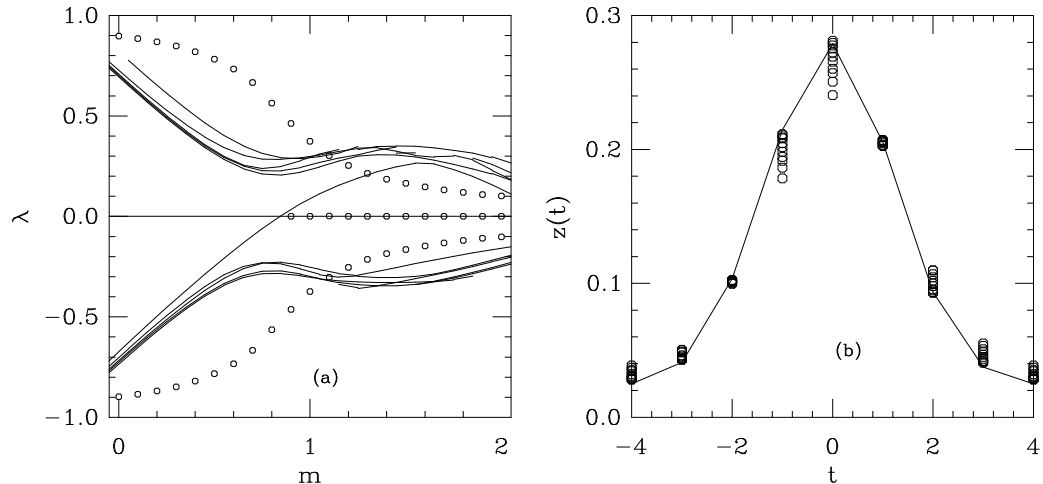


Fig. 3. (a) The low lying spectrum of  $H_o$  (octagons) in a pure SU(2) gauge field background at  $\beta = 2.5$  together with the spectral flow of  $H_w$  (lines). The zero mode of  $H_o$  found for  $m > 0.8$  is singly degenerate and is associated with an instanton in the background gauge field. (b) Shape of the zero mode of  $H_o$  projected to one axis for the various  $m$  (octagons) and of  $H_w$  at the crossing point (line).

both  $H_w(m)$  and  $H_o = \gamma_5 D(0)$  as a function of  $m$  for an SU(2) gauge background at  $\beta = 2.5$  on an  $8^4$  lattice. We see a single level crossing zero near  $m = 0.9$  in the spectral flow of  $H_w$ . At this mass, we see the sudden appearance of a zero eigenvalue (with chirality 1) among the smoothly changing non-zero eigenvalues (in opposite sign pairs with chirality equal to their eigenvalue).

Zero eigenvalues of  $H_o$  due to global topology have a definite chirality. The spectrum of  $H_o$  is in  $[-1,1]$  and the non-zero eigenvalues of  $H_o$  that have a magnitude less than one come in pairs,  $\pm\lambda$ . The associated eigenvectors are not eigenvectors of  $\gamma_5$ , but rather  $\gamma_5$  has expectation value  $\pm\lambda$  in the eigenvectors,  $\psi^\dagger \gamma_5 \psi = \pm\lambda$ . Since  $H_o$  is an even dimensional matrix, the unpaired zero eigenvalues have to be matched by unpaired eigenvalues equal to  $\pm 1$ . This is what is expected to happen in a topologically non-trivial background. It is straightforward to obtain the spectrum of  $D(\mu)$  from the spectrum of  $H_o(0)$ . Due to the continuum like spectrum one can study the approach to the chiral limit using the Overlap-Dirac operator by separating modes due to global topology from the remaining non-zero eigenvalues [8].

The main quantity that needs to be computed numerically is the fermion propagator  $\tilde{D}^{-1}(\mu)$  in Eqn. (5). Certain properties of the Overlap-Dirac operator enable us to compute the propagator for several fermion masses at one time using the multiple Krylov space solver [15] and also go directly to the massless limit.

We note that

$$H_o^2(\mu) = D^\dagger(\mu)D(\mu) = D(\mu)D^\dagger(\mu) = (1 - \mu^2) \left[ H_o^2(0) + \frac{\mu^2}{1 - \mu^2} \right] \quad (15)$$

with

$$H_o^2(0) = \frac{1}{2} + \frac{1}{4} [\gamma_5 \epsilon(H_w) + \epsilon(H_w) \gamma_5] \quad (16)$$

Eq. (15) implies that we can solve the set of equations  $H_o^2(\mu)\eta(\mu) = b$  for several masses,  $\mu$ , simultaneously (for the same right hand  $b$ ) using the multiple Krylov space solver described in Ref. [15]. We will refer to this as the outer conjugate gradient inversion. It is easy to see that  $[H_o^2(\mu), \gamma_5] = 0$ , implying that one can work with the source  $b$  and solutions  $\eta(\mu)$  restricted to one chiral sector.

The numerically expensive part of the Overlap-Dirac operator is the action of  $H_o^2(0)$  on a vector since it involves the action of  $[\gamma_5 \epsilon(H_w) + \epsilon(H_w) \gamma_5]$  on a vector. If the vector  $b$  is chiral (*i.e.*  $\gamma_5 b = \pm b$ ) then,  $[\gamma_5 \epsilon(H_w) + \epsilon(H_w) \gamma_5]b = [\gamma_5 \pm 1]\epsilon(H_w)b$ . Therefore we only need to compute the action of  $\epsilon(H_w)$  on a single vector.

To study the possible onset of spontaneous chiral symmetry breaking in quenched QCD, we stochastically estimate, for a fixed gauge field background,

$$\frac{1}{V} \sum_x \langle \bar{\psi}(x) \psi(x) \rangle_A = \frac{1}{V} \text{Tr}[\tilde{D}^{-1}(\mu)] \quad (17)$$

and average over gauge fields. We also compute stochastically  $\omega = \chi_\pi - \chi_{a_0}$

$$\omega = \frac{2}{V} \langle \text{Tr}(\gamma_5 \tilde{D})^{-2}(\mu) + \text{Tr} \tilde{D}^{-2}(\mu) \rangle = \frac{2}{\mu} \langle \bar{\psi} \psi \rangle - 2 \langle \frac{d}{d\mu} \langle \bar{\psi} \psi \rangle_A \rangle . \quad (18)$$

For a derivation of the above equation we refer the reader to Ref. [8]. Some simple manipulations yield the following relations

$$\begin{aligned} \langle b | \tilde{D}^{-1}(\mu) | b \rangle &= \frac{\mu}{1 - \mu^2} b^\dagger (\eta(\mu) - b) \\ \langle b | (\gamma_5 \tilde{D})^{-2}(\mu) + \tilde{D}^{-2}(\mu) | b \rangle &= \frac{2\mu^2}{(1 - \mu^2)^2} (\eta^\dagger(\mu) - b^\dagger) (\eta(\mu) - b) \end{aligned} \quad (19)$$

where

$$H_o^2(\mu)\eta(\mu) = b \quad \text{with} \quad \gamma_5 b = \pm b . \quad (20)$$

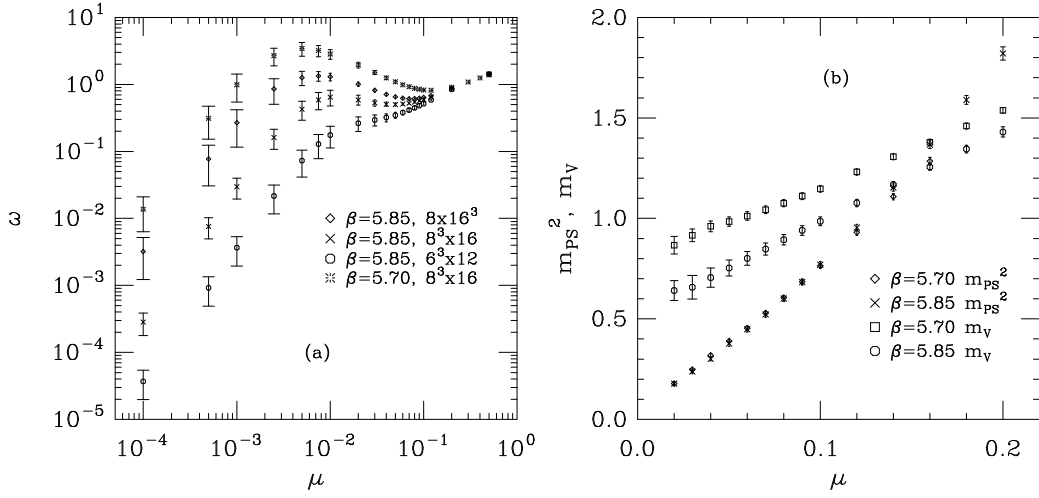


Fig. 4. (a)  $\omega$  without the contribution from global topology as a function of  $\mu$ . (b) The pseudoscalar mass squared,  $am_{PS}^2$ , and the vector mass,  $am_V$ , for  $\beta = 5.85$  and 5.70 on an  $8^3 \times 16$  lattice as a function of  $\mu$ .

As discussed in Ref. [8], it is appropriate to remove the topological contributions to the above quantities in order to study the onset of chiral symmetry breaking. For this we first compute the low lying spectrum of  $\gamma_5 D(0)$  using the Ritz functional method [22]. This gives us, in particular, information about the number of zero modes and their chirality. In gauge fields with zero modes we always find that all  $|Q|$  zero modes have the same chirality. We have not found any accidental zero mode pairs with opposite chiralities. We then perform a stochastic estimate in the chiral sector that has no zero modes and double the result to get the total contribution to  $\langle\bar{\psi}\psi\rangle$  and  $\omega$  excluding topology. In this sector, the propagator is non-singular even for zero fermion mass. Given a Gaussian random source  $b$  with a definite chirality all we have to do is solve the equation  $H_o^2(\mu)\eta(\mu) = b$  for several values of  $\mu$ .

In Fig. 4a we show  $\omega$  without the topology term added for various lattice sizes and  $\beta$  in SU(3) using  $m = 1.65$ . We see some indication of the onset of spontaneous chiral symmetry breaking (with strong finite volume dependence) at  $\beta = 5.85$  where, as  $\mu$  decreases, there is a small region where  $\omega \sim 1/\mu$ , then  $\omega$  turns over and goes like  $\mu^2$ . This latter behavior is expected in finite volume and is obvious from the explicit  $\mu^2$  dependence in Eq. (19).

We show in Fig. 4b pseudoscalar and vector meson masses from a preliminary spectroscopy calculation for SU(3)  $\beta = 5.85$  and 5.70 on an  $8^3 \times 16$  lattice. Masses are extracted using multiple correlation functions in an excited state fit. The fermion masses have been chosen to be above the region of decreasing  $\omega$  from finite volume dependence in Fig. 4a, namely  $\mu > 10^{-2}$ . As in the calculations for  $\omega$  above, a multiple mass shift conjugate gradient solver was

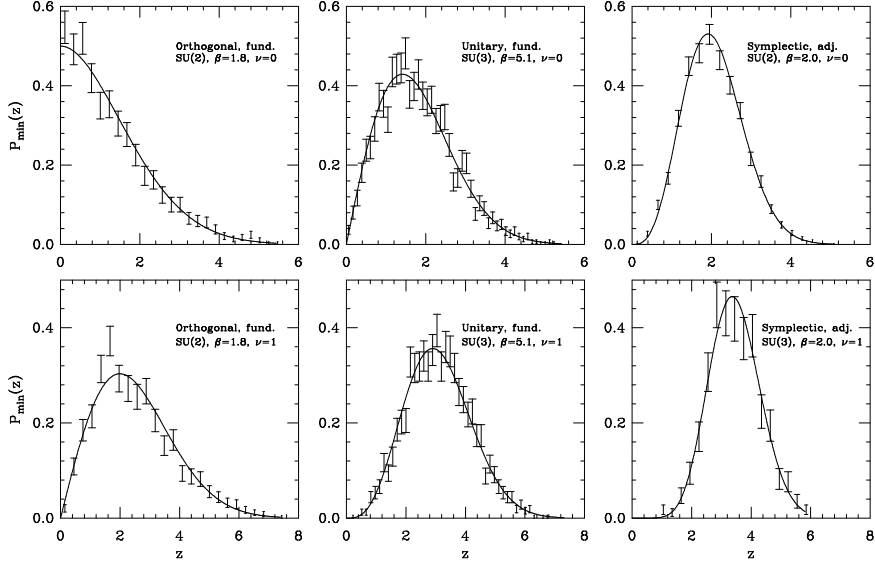


Fig. 5. Plots of the probability distribution,  $P_{\min}(z)$ , of the smallest (rescaled) eigenvalue  $z$  for the orthogonal, unitary and symplectic ensembles in the lowest two topological sectors. Here the smallest eigenvalue  $\lambda$  is rescaled by the volume  $V$  and the infinite volume chiral condensate  $\Sigma$  to  $z = \lambda V \Sigma$ . The curve in each plot is a fit to the prediction from random matrix theory with the best value for the chiral condensate  $\Sigma$ .

used for several values of  $\mu$  in the solution of  $H_o^2(\mu)\eta(\mu) = b$  with chiral source  $b$ . We see some slight deviation of  $am_{PS}^2$  from linearity for decreasing  $\mu$ , and  $am_{PS}^2$  does not extrapolate to 0 at  $\mu = 0$  which we attribute to finite volume dependence. The vector mass  $m_V$  is fairly linear over the entire region.

#### 4 The Overlap-Dirac operator and random matrix theory

The Goldstone pions, associated with the spontaneous breaking of chiral symmetry dominate the low-energy, finite-volume scaling behavior of the Dirac operator spectrum in the microscopic regime, defined by  $1/\Lambda_{QCD} \ll L \ll 1/m_\pi$ , with  $L$  the linear extent of the system. The properties in this regime are universal and can be characterized by chiral random matrix theory (RMT) within three ensembles, depending on some symmetry properties of the Dirac operator, and according to the sector of fixed topology, entering via the number of exact zero modes (see [24] for a recent review). Since the Overlap-Dirac operator has the same chiral properties as the Dirac operator in the continuum, and since it has exact zero modes in topologically non-trivial gauge fields, it is well suited to test the predictions of RMT. In Figure 5 the distribution of the lowest (non-zero) eigenvalue is compared to the predictions of chiral RMT for examples in all three universality classes – SU(2) in the

fundamental representation for the orthogonal ensemble,  $SU(3)$  in the fundamental representation for the unitary ensemble and  $SU(2)$  in the adjoint representation for the symplectic case – and in the sectors with zero or one exact zero modes [25]. Excellent agreement is seen. In addition, the condensate  $\Sigma$  obtained in the two different sectors of each ensemble from fits to the RMT predictions agreed within errors. This agreement further validates the chiral RMT predictions on the one hand and strengthens the case for the usefulness of the overlap regularization of massless fermions on the other hand.

## 5 Conclusions

The Overlap-Dirac operator provides a formulation of vector gauge theories on the lattice with an exact chiral symmetry in the massless limit and no fermion doubling problem. The use of the Overlap-Dirac operator is, however, CPU time intensive. We reviewed a few methods to implement the operator acting on a vector. Of these, we found the optimal rational approximation method, in conjunction with the exact treatment of a few low lying eigenvalues and eigenvectors of  $H_w$  in  $\epsilon(H_w)$ , the most efficient. Further improvements in the numerical treatment of the Overlap-Dirac operator would be very helpful.

The Overlap-Dirac operator has exact zero modes with definite chirality in the presence of topologically non-trivial gauge fields. Due to their good chiral properties overlap fermions are well suited for the study of spontaneous chiral symmetry breaking. It is possible to separate the contribution of the exact zero modes due to topology in a numerical computation. We have presented sample results in a quenched theory from the remaining non-topological modes. We presented first spectroscopy results with overlap fermions in quenched lattice QCD. Finally, we compared the distribution of the smallest eigenvalue of the Overlap-Dirac operator with the predictions from random matrix theory.

## Acknowledgements

The authors would like to thank Herbert Neuberger for useful discussions. This research was supported by DOE contracts DE-FG05-85ER250000 and DE-FG05-96ER40979. Computations were performed on the QCDSF, CM-2, and the workstation cluster at SCRI, and the Xolas computing cluster at MIT’s Laboratory for Computing Science.

## References

- [1] R. Narayanan and H. Neuberger, *Nucl. Phys.* **B443** (1995) 305.
- [2] D.B. Kaplan, *Phys. Lett.* **B288** (1992) 342; S.A. Frolov and A.A. Slavnov, *Phys. Lett.* **B309** (1993) 344.
- [3] R. Narayanan, H. Neuberger and P. Vranas, *Phys. Lett.* **B353** (1995) 507; Y. Kikukawa, R. Narayanan and H. Neuberger, *Phys. Rev.* **D57** (1998) 1233.
- [4] H. Neuberger, hep-lat/9807009; hep-lat/9808036 for recent reviews.
- [5] Y. Shamir, *Nucl. Phys.* **B406** (1993) 90; V. Furman and Y. Shamir, *Nucl. Phys.* **B439** (1995) 54.
- [6] H. Neuberger, *Phys. Rev.* **D57** (1998) 5417.
- [7] H. Neuberger, *Phys. Lett.* **B417** (1998) 141.
- [8] R.G. Edwards, U.M. Heller and R. Narayanan, hep-lat/9811030 to appear in *Phys. Rev. D*.
- [9] F. Niedermeyer, hep-lat/9810026 and references therein.
- [10] P.H. Ginsparg and K.G. Wilson, *Phys. Rev.* **D25** (1982) 2649.
- [11] R. Narayanan, *Phys. Rev.* **D58** (1998) 097501.
- [12] G.H. Golub and C.F. van Loan, “Matrix Computations”, The Johns Hopkins University Press, 1983. For an implementation in this context see T.W. Chiu, *Phys. Rev.* **D58** (1998) 074511.
- [13] B. Bunk, *Nucl. Phys. Proc. Suppl.* **B63** (1998) 952.
- [14] R.G. Edwards, U.M. Heller and R. Narayanan, *Nucl. Phys.* **B540** 457.
- [15] A. Frommer, S. Güskens, T. Lippert, B. Nöckel, K. Schilling, *Int. J. Mod. Phys.* **C6** (1995) 627; B. Jegerlehner, hep-lat/9612014.
- [16] N.J. Higham, Linear Algebra and Appl., Proceedings of ILAS Conference “Pure and Applied Linear Algebra: The New Generation”, Pensacola, March 1993.
- [17] H. Neuberger, *Phys. Rev. Lett.* **81** (1998) 4060.
- [18] E. Ya. Remez, *General Computational Methods of Chebyshev Approximations. The Problems of Linear Real Parameters*, AEC-tr-4491, U.S. Atomic Energy Commission, 1962; S.L. Moshier, *Methods and Programs for Mathematical Functions*, Halsted Press, New York, 1989. Code available from <http://www.netlib.org/cephes/remes.shar> .
- [19] H. Neuberger, hep-lat/9811019.
- [20] A. Borici, hep-lat/9810064.

- [21] R.G. Edwards, U.M. Heller and R. Narayanan, *Nucl.Phys.* **B535** (1998) 403; hep-lat/9901015 (to be published in Phys. Rev. D.); R.Narayanan, hep-lat/9810045.
- [22] B. Bunk, K. Jansen, M. Lüscher and H. Simma, DESY-Report (September 1994); T. Kalkreuter and H. Simma, *Comput. Phys. Commun.* **93** (1996) 33.
- [23] P. Chen, N. Christ, G. Fleming, A. Kaehler, C. Malureanu, R. Mawhinney, G. Siegert, C. Sui, P. Vranas and Y. Zhestkov, hep-lat/9812011, T. Blum, hep-lat/9810017.
- [24] J.J.M. Verbaarschot, hep-ph/9902394.
- [25] R.G. Edwards, U.M. Heller, J. Kiskis and R. Narayanan, hep-th/9902117.